Icarus 245 (2015) 153–161

Contents lists available at ScienceDirect

Icarus

journal homepage: www.elsevier.com/locate/icarus

Laboratory measurements of the 3.7–20 cm wavelength opacity of sulfur dioxide and carbon dioxide under simulated conditions for the deep atmosphere of Venus

Paul G. Steffes *, Patrick Shahan, G. Christopher Barisich, Amadeo Bellotti

School of Electrical and Computer Engineering, Georgia Institute of Technology, Atlanta, GA 30332-0250, United States

ARTICLE INFO

Article history:
Received 7 June 2014
Revised 9 September 2014
Accepted 9 September 2014
Available online 28 September 2014

Keywords:
Venus, atmosphere
Radio observations
Atmospheres, composition
Spectroscopy

ABSTRACT

In the past two decades, multiple observations of Venus have been made at X-Band (3.6 cm) using the Jansky Very Large Array (VLA), and maps have been created of the 3.6 cm emission from Venus (see, e.g., Devaraj, K. [2011]. The Centimeter- and Millimeter-Wavelength Ammonia Absorption Spectra under Jovian Conditions. PhD Thesis, Georgia Institute of Technology, Atlanta, GA). Since the emission morphology is related both to surface features and to deep atmospheric absorption from CO_2 and SO_2 (see, e.g., Butler, B.J., Steffes, P.G., Suleiman, S.H., Kolodner, M.A., Jenkins, J.M. [2001]. Icarus 154, 226–238), knowledge of the microwave absorption properties of sulfur dioxide in a carbon dioxide atmosphere under conditions for the deep atmosphere of Venus is required for proper interpretation. Except for a single measurement campaign conducted at a single wavelength (3.2 cm) over 40 years ago (Ho, W., Kaufman, I.A., Thaddeus, P. [1966]. J. Geophys. Res. 71, 5091–5108), no measurements of the centimeter-wavelength properties of any Venus atmospheric constituent have been conducted under conditions characteristic of the deep atmosphere (pressures from 10 to 92 bars and temperatures from 400 to 700 K). New measurements of the microwave properties of SO_2 and CO_2 at wavelengths from 3.7 to 20 cm have been conducted under simulated conditions for the deep atmosphere of Venus, using a new high-pressure system. Results from this measurement campaign conducted at temperatures from 430 K to 560 K and at pressures up to 92 bars are presented. Results indicate that the model for the centimeter-wavelength opacity from pure CO_2 (Ho, W., Kaufman, I.A., Thaddeus, P. [1966]. J. Geophys. Res. 71, 5091–5108), is valid over the entire centimeter-wavelength range under simulated conditions for the deep atmosphere of Venus. Additionally, the laboratory results indicate that both of the models for the centimeter-wavelength opacity of SO_2 in a CO_2 atmosphere from Suleiman et al. (Suleiman, S.H., Kolodner, M.A., Steffes, P.G. [1996]. J. Geophys. Res. 101, 4623–4635) and from Fahd and Steffes (Fahd, A.K., Steffes, P.G. [1992]. Icarus 97, 200–210) can reliably be used under conditions of the deep atmosphere of Venus.

1. Introduction

It is well understood that the microwave emission spectrum of Venus reflects the abundance and distribution of constituents such as carbon dioxide, sulfur dioxide, and sulfuric acid vapor (see, e.g., Steffes et al., 1990), but there are a number of factors that limit the accuracy of this approach for microwave remote sensing of these constituents. The most critical of these is the knowledge of the microwave absorption properties of these constituents under Venus atmospheric conditions. While the microwave absorption properties of both gaseous sulfuric acid vapor and sulfur dioxide in a carbon dioxide atmosphere have been measured and modeled at pressures up to 6 bars (Kolodner and Steffes, 1998, Suleiman et al., 1996; Fahd and Steffes, 1992), no measurements of the centimeter-wavelength properties of any Venus atmospheric constituent have been conducted under conditions characteristic of the deep atmosphere (pressures from 10 to 92 bars and temperatures from 400 to 700 K), excepting a single measurement campaign conducted at a single wavelength (3.2 cm) over 40 years ago (Ho et al., 1966). At altitudes below 35 km, H_2SO_4 thermally dissociates, forming H_2O and SO_3, both of which exhibit very small amounts of microwave absorption at the abundance levels present in the Venus atmosphere (Ho et al., 1966; Steffes and Eshleman, 1981). Thus, in the deep atmosphere, only SO_2 and CO_2 have the potential to affect the observed microwave emission.

* Corresponding author. Fax: +1 404 894 5935.
E-mail address: steffes@gatech.edu (P.G. Steffes).

http://dx.doi.org/10.1016/j.icarus.2014.09.012
0019-1035/

Microwave observations of Venus were conducted in 1996 at 4 wavelengths using the NRAO Very Large Array (Butler et al., 2001). Maps of emission from Venus were made at two of the wavelengths (1.3 cm and 2.0 cm), which indicated dark (~3%) polar regions consistent with increased sulfuric acid vapor abundance due to vaporization of cloud condensate from the downwelling characteristic of Hadley cell circulation (Jenkins et al., 2002). Over the disk of Venus, the weighting functions at these wavelengths peak well above the surface or boundary layer (Jenkins et al., 2002). As shown in Fig. 1, even at the disk center (nadir) with the deepest possible weighting functions, the emission at wavelengths of 2 cm and shorter largely originates from altitudes above the boundary layer (0–10 km). At 3.6 cm, emission from both the boundary layer and surface are present. Devaraj (2011) made maps of the 3.6 cm emission from Venus based both on the 1996 observations (Butler et al., 2001) and from subsequent observations conducted in 2009 from the NRAO Very Large Array. Since variations in 3.6 cm emission are due both to variations in surface emissivity and potentially from variability in the abundance of SO_2 in the boundary layer, accurate interpretation of such data requires accurate models of the microwave opacity of constituents in the boundary layer.

In this paper, we report new measurements of the microwave properties of SO_2 and CO_2 at wavelengths from 3.7 to 20 cm that have been recently completed under simulated conditions for the deep atmosphere of Venus, using a new high-pressure system. Results from this measurement campaign conducted at temperatures from 430 K to 560 K and at pressures up to 92 bars are presented. Results indicate that the model for the centimeter-wavelength opacity of pure CO_2 (Ho et al., 1966), is valid over the entire centimeter-wavelength range under simulated conditions for the deep atmosphere of Venus. Additionally, the laboratory results indicate that the models for the centimeter-wavelength opacity of SO_2 in a CO_2 atmosphere from Suleiman et al. (1996) and from Fahd and Steffes (1992) can reliably be used under conditions of the deep atmosphere of Venus.

2. Measurement theory and system

In our new laboratory measurement campaign conducted for pure CO_2, nearly 100 laboratory measurements of microwave opacity were made in the pressure range from 20 to 80 bars, at temperatures of 435 and 495 K, and at wavelengths from 3.7 to 20 cm (1.5–8.2 GHz). For the opacity of SO_2 in a CO_2 atmosphere, we conducted 120 new laboratory measurements in the pressure range from 4 to 92 bars; at temperatures of 435 K, 495 K, and 560 K; and at wavelengths from 3.7 to 20 cm (1.5–8.2 GHz). The mole fraction of sulfur dioxide ranged from 0.2% to 7.4% with some additional measurements of pure SO_2. In order to conduct experiments under the extreme conditions characteristic of the deep Venus atmosphere, a new laboratory measurement system, initially developed to simulate the deep jovian atmosphere (Karpowicz and Steffes, 2011), was modified so as to simulate Venus conditions. The method used to measure the microwave absorptivity of a gas is based on the lessening in the quality factor (Q) of a resonant mode of a cylindrical cavity in the presence of a lossy gas. This technique involves monitoring the changes in Q of different resonances of a cavity resonator in order to determine the refractive index and the absorption coefficient of an introduced gas or gas mixture (at those resonant frequencies). Described at length by Hanley and Steffes (2007), it has been successfully utilized for over one half of a century.

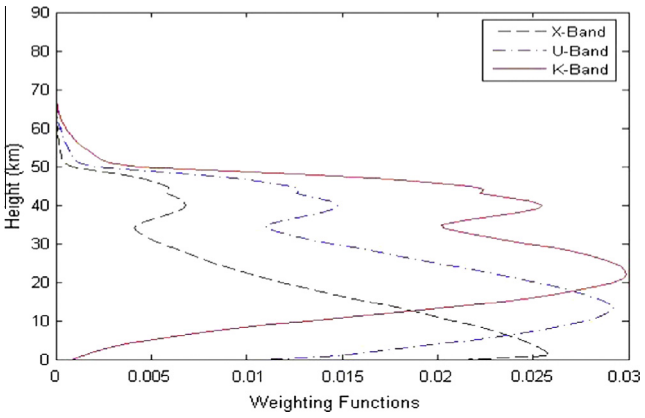

Fig. 1. Weighting functions for center of Venus disk at 3.6 cm (X-Band), 2 cm (U-Band) and 1.3 cm (K-Band), from Steffes et al. (2013).

2.1. Laboratory configuration

Shown in Fig. 2 is a block diagram of the measurement system used for these measurements. Fig. 2a shows the gas handling system used to create the gas mixtures under simulated Venus conditions. Fig. 2b shows the data acquisition system necessary to monitor the environmental conditions of the gases under test and the microwave system used to measure their microwave properties. The heart of the gas handling system is the pressure vessel that contains the microwave resonator which is used to characterize the microwave properties of the gases under test.

The pressure vessel was built by Hays Fabrication and Welding (Springfield, Ohio). The vessel is constructed from a 30.48 cm section of schedule 100 pipe that is 35.56 cm in diameter (outer dimension). An elliptical head is welded to the bottom giving the vessel a maximum interior height of 46.04 cm (19 in.). The top includes an ANSI class 900 flange 10.16 cm (4 in.) thick, with a top plate that is 9.2 cm (3–5/8 in.) thick. The vessel has an interior volume of 32.75 l, and weighs approximately 544.3 kg. A composite (glass fiber/NBR) KLINGERsil C-4430 gasket is used to seal the pressure vessel along with 20 nuts, each 6 cm in diameter, torqued to 62 Newton-meters.

The system includes a Grieve industrial oven model AB-650 (maximum temperature 616 K), along with pressure gauges (one rated from 0 to 2 bars absolute, the other rated to 20 bars), an Omega RPX1009L0-1.5KAV pressure transducer capable of measuring up to 103 bars (at temperatures up to 588 K), and a high precision resistance temperature detector (RTD) (Omega model PRCU-10-2-100-1/4-9-E). Valves rated for high temperature and pressure were used throughout the system. The system is placed upon an outdoor concrete pad. Thus, all system components except for the microwave network analyzer, sensor monitors, and the control computer are placed outdoors, protected by a metallic shed. Certified UHP grade carbon dioxide, methane, and sulfur dioxide cylinders from Airgas, Inc. were used for the test gas and dielectric matching measurements.

The microwave resonator included in Fig. 2b has been used in several studies. Its most recent version was described in Hanley and Steffes (2007). The resonator is a cylindrical cavity resonator with an interior height of 25.75 cm, and an interior radius of 13.12 cm. The resonator is connected to the network analyzer via high temperature coaxial cables and via Ceramtec (16545-01-CF) coaxial bulkhead feedthroughs capable of maintaining pressures up to 103 bars at temperatures up to 623 K. Outside of the oven, two sections of Andrews CNT 600 microwave cable (each 24 m in length) connect to the Agilent R E5071C network analyzer, located in a stable, indoor environment. The S parameters measured by the network analyzer, related to the quality factor (Q) and center

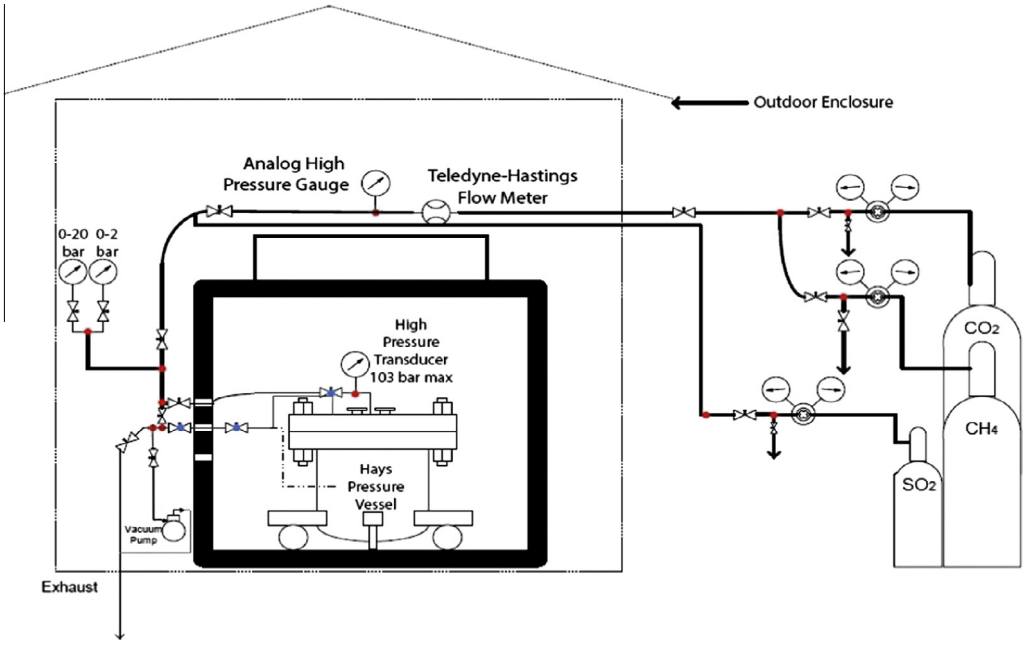

Fig. 2a. Gas handling system for the ultra-high pressure simulator.

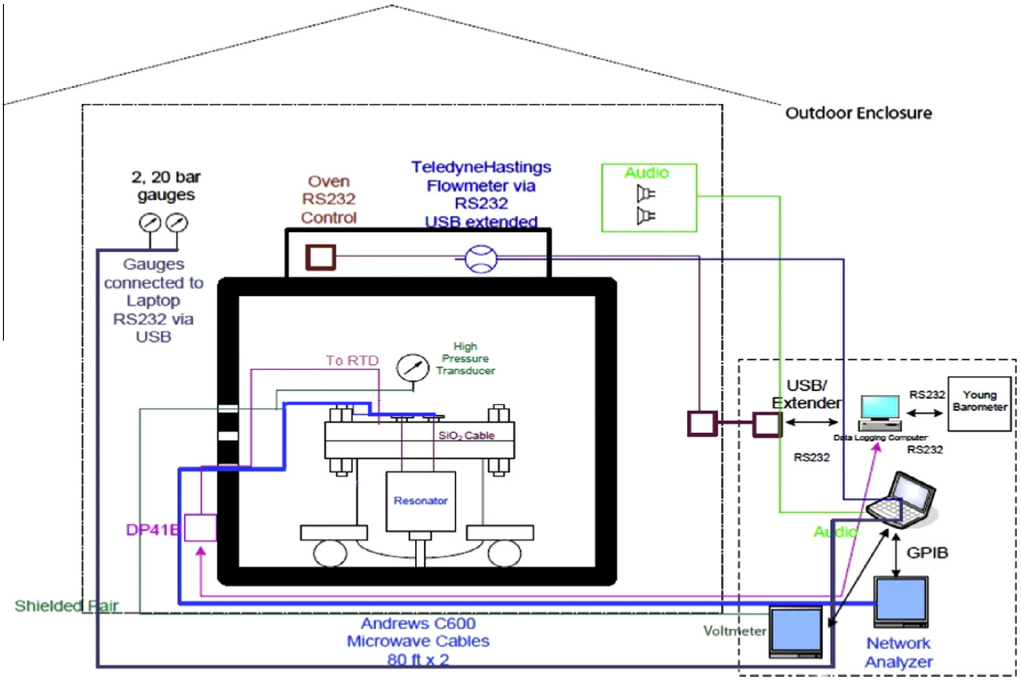

Fig. 2b. Microwave/electronic measurement system.

frequency of each resonance, are read in via a General Purpose Interface Bus (GPIB) to the data acquisition computer.

2.2. Measurement theory

The microwave absorption of a gas introduced into a resonator is determined through measurement of the lessening in the quality factor of the individual resonances in the presence of the lossy gas (see, e.g., Hanley and Steffes, 2007). The quality factor, or Q, of each resonance, is defined as (Matthaei et al., 1980)

$$Q = \frac{2\pi f_0 \times Energy\ Stored}{Average\ Power\ Loss} \tag{1}$$

with f_0 being the center frequency of the resonance. The quality factor, Q, of each resonance is directly measured by dividing the measured center frequency by the measured half-power bandwidth (HPBW)

$$Q = \frac{f_0}{HPBW} \tag{2}$$

The absorptivity, α of the gas is related to its $Q(\varepsilon'/\varepsilon'')$ by

$$\alpha \approx \frac{\varepsilon'' \pi}{\varepsilon' \lambda} = \frac{1}{Q_{gas}} \frac{\pi}{\lambda} \tag{3}$$

where ε' and ε'' represent the real and imaginary components of the gas' permittivity, respectively, λ is the wavelength expressed in km and the resulting opacity α is in the units of Nepers/km (note that 1 Neper = 8.686 dB). The quality factor of a resonator loaded with a lossy test gas is given by

$$\frac{1}{Q^m_{loaded}} = \frac{1}{Q_{gas}} + \frac{1}{Q_r} + \frac{1}{Q_{ext1}} + \frac{1}{Q_{ext2}} \tag{4}$$

with Q^m_{loaded} being the measured quality factor of the loaded resonator, Q_{gas} being the quality factor of the gaseous medium under investigation, Q_r being the quality factor of the evacuated cavity resonator without coupling losses and both Q_{ext1} and Q_{ext2} being the external coupling losses of the resonator's coupling probes. Consistent with Hanley and Steffes (2007), Q_{ext1} is assumed equivalent to Q_{ext2} since a symmetrical resonator is used to collect laboratory measurements in this work. The transmissivity can be used to calculate the coupling losses Q_{ext} and is given by

$$t = 10^{-S/10} \tag{5}$$

where S is the insertion loss (in dB) of the resonator at the center frequency of a given resonance (Matthaei et al., 1980). The relationship between the value for transmissivity and the coupling losses is described as

$$t = \left[\frac{2Q^m}{Q_{ext}}\right]^2 \tag{6}$$

and solving for the coupling losses gives

$$Q_{ext} = \frac{2Q^m}{\sqrt{t}} \tag{7}$$

where Q^m is the measured quality factor. The measured quality factor of the resonator at vacuum Q^m_{vac} is related to Q_r by

$$\frac{1}{Q^m_{vac}} = \frac{1}{Q_r} + \frac{1}{Q_{ext1}} + \frac{1}{Q_{ext2}} \tag{8}$$

Substituting the relationship for Q_{ext} into the equation for Q^m_{vac} and Q^m_{loaded} gives

$$\frac{1}{Q_{gas}} = \frac{1-\sqrt{t_{loaded}}}{Q^m_{loaded}} - \frac{1-\sqrt{t_{vac}}}{Q^m_{vac}} \tag{9}$$

where t_{loaded} and t_{vac} represent the transmissivity at loaded and vacuum conditions respectively. The magnitude of the shift in the peak frequencies of the resonances depends on the abundance and refractive index of the gas present. Even in the presence of a lossless gas, the quality factor can change along with the center frequency due to the variations in the coupling losses with resonant frequency; this effect is known as dielectric loading (see, e.g., DeBoer and Steffes, 1994). The dielectric loading effect can be mitigated by shifting the desired resonance by the same amount as that of the test gas using a lossless gas, and taking additional measurements of the quality factor and transmissivity under those conditions. These dielectric matching measurements replace Q^m_{vac} and t_{vac} to give the final equation for calculating the opacity. The relationship for absorptivity is converted from the units of Nepers/km into dB/km (1 Neper/km = 8.686 dB/km) and is given by

$$\alpha = 8.686 \frac{\pi}{\lambda} \left(\frac{1-\sqrt{t_{loaded}}}{Q^m_{loaded}} - \frac{1-\sqrt{t_{matched}}}{Q^m_{matched}} \right) \text{ (dB/km)} \tag{10}$$

It is also important to know the refractive index n_{ri} of the gas under test since small changes in this value could alter the way the electromagnetic waves propagate through the medium. Although n_{ri} is known to be very close to unity for most gases, the frequency shift exhibited by the resonances can be used to determine this refractive index to a high level of accuracy. The refractivity (N) is given by

$$N = 10^6 (n_{ri} - 1) \tag{11}$$

The refractivity is measured by comparing the center frequency of the resonances under gaseous conditions to the peak frequency of the resonances at vacuum and is given by

$$N = \frac{10^6 (f_{vac} - f_{gas})}{f_{gas}} \tag{12}$$

where N is the refractivity of the entire gas mixture, f_{gas} is the peak frequency of the resonance in the presence of the test gas and f_{vac} is the peak frequency of the resonator at vacuum (Tyler and Howard, 1969). The overall refractivity of the mixture is the sum of the refractivity of the individual gases scaled with their respective mole fractions.

2.3. Measurement procedure

When initiating measurements, system integrity is verified by assuring that the outdoor gas containment system has no leaks. This assures that any toxic or flammable gas does not escape to the surrounding atmosphere and also reduces uncertainties associated with constituent partial pressures. The pressure vessel is sealed at low temperatures so that the seal will improve as the sealant material expands at higher temperatures and ensures that the pressure vessel remains leak-proof.

Since it is easier to make changes to the mixing ratio and pressure of gases in the pressure vessel than to change the temperature of the system, sets of measurements are taken at a particular temperature with multiple pressures, concentrations and mixing ratios before measurements at a different temperature are taken. Once all measurements are completed at one temperature, the set point for the oven is adjusted to bring the temperature chamber to a new temperature for the subsequent experiments.

Measurements of the centimeter-wavelength opacity of pure CO_2 begin by conducting measurements of the available microwave resonances (twelve frequencies from 1.5 to 8.2 GHz, or wavelengths from 3.6 to 20 cm) under vacuum conditions at the desired temperature. The next step is to add the test gas (carbon dioxide) to the system. Once it is thermally stabilized, which can take several hours due to the outdoor system's large volume and large thermal time constant, measurements of the center frequency and quality factor of each resonance are taken 30 times and averaged. Subsequent measurements are conducted using several different pressures of carbon dioxide, and then a second vacuum is drawn. A second set of vacuum measurements are taken at the desired temperature. The dielectric matching process consists of shifting the resonances by the same amount as that of the test gas using a highly refractive and microwave transparent gas (in this case, methane). The selection of methane was driven by its high refractivity (similar to that of carbon dioxide) and microwave transparency (Chinsomboon, 2012), which allowed for dielectric matching without exceeding the pressure capabilities of the chamber. Measurements of the quality factors of each resonance are recorded as dielectric matches are made with the reference gas. Finally, a third and final vacuum is drawn in the system so as to evacuate the matching gas, and the necessary measurements of center frequency and quality factor of each resonance are taken. Following this step, three sets of straight-through measurements of the signal levels are made. This is achieved by detaching the RG-214 cables from the Ceramtec® feedthroughs and connecting them directly to each other (without the presence of the resonator) through a high-temperature female-to-female BNC connector. The three sets of transmissivity measurements are taken at the

standard resonant frequencies. The purpose of taking straight-through measurements is to quantify the losses in the cables and to correct for transmissivities in both the loaded and matched measurements. The coax connections are disconnected and reconnected between each set of transmissivity measurement in order to better statistically characterize the reproducibility of the electrical connections (Devaraj, 2011). The process of collecting transmissivity measurements includes opening the industrial oven door to disconnect and reconnect the cables and may result in a temporary temperature variation. Thus, all transmissivity measurements are taken at the end of the experiment set to ensure that the resonator remains at a constant temperature, within the ±0.1 °C margin.

For measurements involving sulfur dioxide, a polar molecule, the potential for significant adsorption of SO_2 by the metallic surfaces was not considered likely, because of the high temperatures involved. However, a method was employed to compensate for any possible adsorption effect by saturating the surface of the gas handling system with a layer of sulfur dioxide before the measurements are taken. (A similar approach was employed by Hanley et al. (2009) for their measurements of ammonia.) Since only a limited number of adsorbate layers can form, any additional gas added would not adsorb after the substrate surface is fully saturated. The adsorption of sulfur dioxide is monitored by measuring changes in the quality factors of the resonances with time. Once the quality factors stabilize, the internal surface is said to be fully saturated, at which point, the rate of adsorption and desorption is equal. Only after the sulfur dioxide abundance is stable are measurements taken, and then the pressure-broadening carbon dioxide is added to the system. As with the measurements for pure carbon dioxide, the first set of measurements of the available resonances is taken under vacuum conditions at the desired temperature. The next step is to add the primary test gas (sulfur dioxide). Once the system is thermally stabilized and the necessary measurements are taken, carbon dioxide is added as the broadening gas. The frequency shifted resonances are then again measured. After measurements are conducted by adding several different pressures of carbon dioxide, a second vacuum is drawn. After venting down to atmospheric pressure, the vacuum pump is run for at least 12 h to ensure that the remaining test gases have been evacuated. A second set of vacuum measurements are taken at the desired temperature. The dielectric matching process consists of shifting the resonances by the same amount as that of the test gas mixture using pure carbon dioxide. Measurements of the quality factors of each resonance are recorded as dielectric matches are made with the reference gas. Since the broadening gas (CO_2) exhibits it own collisionally-induced microwave absorption (measured directly as described above), using carbon dioxide as the matching gas makes possible the separation of the absorption due only to SO_2 from that of the aggregate SO_2/CO_2 mixture. By conducting *differential* measurements of the resonator quality factors between the SO_2/CO_2 mixture and an equivalent density of pure CO_2, it is possible to measure the pressure-broadened opacity due only to SO_2. Finally, a third and final vacuum is drawn in the system so as to evacuate the matching gas, and the necessary measurements of center frequency and quality factor of each resonance are taken. Following this step, three sets of straight-through measurements of the signal levels are made as described above for the measurements of pure carbon dioxide.

2.4. Measurement uncertainties

As discussed extensively by Hanley and Steffes (2007) and by Karpowicz and Steffes (2011), the uncertainties associated with these centimeter-wavelength opacity measurements are associated with 5 different types of errors. These uncertainties arise from instrumentation errors and electrical noise (Err_{inst}), errors in dielectric matching (Err_{diel}), errors in measured transmissivity (Err_{trans}), errors due to asymmetry in resonances (Err_{asym}) and errors from uncertainties in the measured environmental conditions (Err_{cond}). Instrumentation errors arise from both the limited sensitivity of the electrical system and the ability of the system to accurately measure bandwidths ($BW_{measured}$) and peak frequencies (f_0). Errors in dielectric matching arise from small mismatches in the alignment of the center frequencies of the test and matching gas. Transmissivity errors are caused by uncorrected losses in the electronics, cables, adapters and waveguides in the system. This ultimately translates into an uncertainty in the power amplitude of the measurement of each resonance. The asymmetry errors are a result of the asymmetric nature of the resonances due to the overlapping of nearby undesired resonances. Lastly, the errors due to experimental conditions arise from uncertainties in the measured pressure, temperature and concentration. Err_{cond} does not directly affect the opacity measurements, but plays a crucial role in using the measurements to evaluated the accuracy of a microwave opacity model. Of the various sources of errors introduced here, errors in dielectric matching are the least statistically significant due to the high accuracy of the data collection software while taking the loaded and matched measurements.

Both noise of electronic components and the accuracies of the frequency references contribute to Err_{inst}. The contribution of noise to the instrumental uncertainty is calculated by evaluating the statistics of the measurements of resonance center frequency and bandwidth over multiple measurements. This is done as outlined in Hanley et al. (2009),

$$Err_n = B \times \frac{S_n}{\sqrt{n_{samples}}} \tag{13}$$

where S_n is the sample standard deviation, B is the confidence coefficient and $n_{samples}$ is the number of independent measurements taken of the sample. The data collection system is configured to collect 30 sets of independent measurements for each resonance. The confidence coefficient B depends on the confidence interval used. In this work, a 95% confidence interval (approximately 2σ) is employed. The confidence coefficient is equivalent to the critical value of a Student t-test with a two-tailed significance of 0.05 and $(n_{samples} - 1)$ degrees of freedom (Student, 1908). A 95% confidence interval means that the actual average will be in the range above the interval 2.5% of the time, and 2.5% of the time below, for a total uncertainty of 5%. For 30 samples, the confidence coefficient is 2.045. S_n consists of only the standard deviation of the resonances' bandwidth because the standard deviation of the center frequencies is extremely small and its effects on the quality factors is negligible.When calculating Err_{inst}, the systematic instrumental error in measuring the center frequency of resonance (Err_o) and the systematic instrumental error in measuring the bandwidth of resonance Err_{BW} are also computed and then integrated into the error as per Hanley et al. (2009).

Uncertainties resulting from imperfect dielectric matching, transmissivity and resonance asymmetry are also computed in the same fashion as Hanley et al. (2009) and Karpowicz and Steffes (2011). Dielectric mismatches and small misalignments of the center frequencies between the loaded and matched conditions give rise to errors in dielectric matching (Err_{diel}). Although the matching gas for measurements of pure CO_2 (methane) is lossless, the measured quality factor can still vary slightly from those measured at vacuum. For matching the SO_2/CO_2 mixtures, pure CO_2 is used, and thus the measured quality factor is significantly different than that at vacuum. Through the comparison of the Qs of the three vacuum measurements, this effect can be taken into account

$$\left(\frac{dQ}{df}\right)_i = \left|\frac{Q_{vac,i} - Q_{matched}}{f_{vac,i} - f_{matched}}\right| \quad i = 1, 2 \text{ and } 3 \tag{14}$$

The dQ is then calculated using the maximum of the three values

$$dQ = \left(\frac{dQ}{df}\right)_{max} |f_{loaded} - f_{matched}| \quad (15)$$

with f_{loaded} being the frequency of the resonance when under loaded conditions and $f_{matched}$ being the frequency of the resonance when under matching conditions. The uncertainties of microwave opacity measurements due to dielectric mismatches can then be calculated as

$$Err_{diel} = \frac{8.686\pi}{\lambda} \times \left| \left(\frac{1-\sqrt{t_{loaded}}}{Q^m_{loaded}} - \frac{1-\sqrt{t_{matched}}}{Q^m_{matched}+dQ} \right) - \left(\frac{1-\sqrt{t_{loaded}}}{Q^m_{loaded}} - \frac{1-\sqrt{t_{matched}}}{Q^m_{matched}-dQ} \right) \right| \quad (\mathrm{dB/km}) \quad (16)$$

Uncertainties in transmissivity are related to limited knowledge of losses in the microwave instruments and other equipment (including the Vector Network Analyzer, cables, and adapters). This error is reflected by the uncertainty of the measured amplitude. A major source of error is the repeatability of cable connections which can be characterized by disconnecting and reconnecting the cables during transmissivity measurements. It should be noted that since the same cables are used to couple all resonances, such errors due to limited repeatability will be correlated between resonances. The RG-214 cables connected to the pressure vessel feedthroughs are disconnected and connected together in a thru-configuration through a high-temperature female-to-female BNC connector. The signal level measurements are taken thrice to generate three measurement samples. The cables are disconnected and reconnected together again between each set of measurement. The error in the measured signal level is given by

$$Err_{msl} = \frac{4.303}{\sqrt{3}} S_n \quad (17)$$

where S_n is the standard deviation of the sample cable loss measurements expressed in dB. The confidence coefficient of 4.303 is equal to the critical value of the 3-sample Student t-test at the 95% confidence interval (Student, 1908). Err_{msl} only takes into account the performance variations of the cables outside the pressure vessel which can be disconnected and reconnected but not the portion of the SiO_2 cable that lies within the pressure vessel. Therefore, an additional 0.25 dB is added to account for the worst-case variations in cable performance (Karpowicz and Steffes, 2011). Moreover, an additional 0.5 dB is also included in order to reflect variations in cable losses due to temperature fluctuations in the 15 m long outdoor section of the two 24.4 m long Andrews® CNT 600 microwave cables. The resulting uncertainty in the insertion loss of the system is given as

$$Err_{ins\ loss} = \sqrt{Err_{msl} + 0.25^2 + 0.5^2} \quad (\mathrm{dB}) \quad (18)$$

The insertion loss is related to transmissivity error through the following relationship

$$Err_{t,i} = \frac{1}{2}\left(10^{-(S_i - Err_{ins\ loss})} - 10^{-(S_i + Err_{ins\ loss})}\right) \quad i = l, m \quad (19)$$

where the subscripts l and m represents the loaded and matched conditions respectively. S represents the resonator's insertion loss. The 2σ uncertainties in microwave opacity due to transmissivity are given by

$$Err_{trans} = \frac{8.686\pi}{2\lambda}\left(\frac{\sqrt{t_l + Err_{t,l}} - \sqrt{t_l - Err_{t,l}}}{Q^m_{loaded}} - \frac{\sqrt{t_m - Err_{t,m}} - \sqrt{t_m + Err_{t,m}}}{Q^m_{matched}} \right) \quad (\mathrm{dB/km}) \quad (20)$$

The asymmetric nature of the measured resonances also contributes to the overall uncertainty of microwave opacity. The asymmetry is a result of off-axis/TM mode resonances overlapping the axial/TE mode resonances. This uncertainty arises when loaded measurements experience disproportionate asymmetric broadening as compared to the matched measurements. This effect is more noticeable at lower temperatures and shorter wavelengths. The calculation of the bandwidth based on the higher and lower halves of each resonance characterizes the asymmetric nature of the resonances

$$BW_{high} = 2 \times (f_{high} - f_{center}) \quad (21)$$

$$BW_{low} = 2 \times (f_{center} - f_{low}) \quad (22)$$

where BW_{high} and BW_{low} are full bandwidths based on the high and low sides of the resonance, f_{high} is the upper half-power frequency, f_{center} is the center frequency of the resonance and f_{low} is the lower half-power frequency. In order to characterize the error, the resulting opacities are calculated with BW_{high} and BW_{low} values. The difference in microwave opacity between the two calculations is regarded as the 2σ errors. Thus, the uncertainty due to resonance asymmetry is expressed as

$$Err_{asym} = \frac{8.686\pi}{\lambda} \times \left| \left(\frac{1-\sqrt{t_{loaded}}}{Q^m_{loaded,high}} - \frac{1-\sqrt{t_{matched}}}{Q^m_{matched,high}} \right) - \left(\frac{1-\sqrt{t_{loaded}}}{Q^m_{loaded,low}} - \frac{1-\sqrt{t_{matched}}}{Q^m_{matched,low}} \right) \right| \quad (\mathrm{dB/km}) \quad (23)$$

where $Q^m_{loaded,high}$ and $Q^m_{loaded,low}$ are the computed quality factors for the loaded condition calculated with the high and low halves of the resonance, respectively. $Q^m_{matched,high}$ and $Q^m_{matched,low}$ are the computed quality factors for the matched condition calculated with the high and low halves of the resonance, respectively. Thus, as per Hanley et al. (2009), the 95% confidence measurement uncertainty (Err_{tot}) is given in dB/km as

$$Err_{tot} = \sqrt{Err^2_{inst} + Err^2_{diel} + Err^2_{trans} + Err^2_{asym}} \quad (24)$$

At the highest temperature used in our experiments (560 K), the measurement uncertainty becomes significantly larger due to reductions in the signal-to-noise in the system resulting from increased cable opacity within the oven.

Uncertainty due to experimental conditions (Err_{cond}) takes into account the uncertainties in temperature, pressure and concentration of the gas mixture under test. (Table 1 shows all instrumentation used in determination of test conditions, and the accompanying uncertainties.) Although it does not directly affect the uncertainty of the measured microwave opacity, inclusion of the effects of uncertainties in test conditions is necessary for accurate assessment of opacity models. The calculation of Err_{cond} is given as

$$Err_{cond} = \sqrt{Err^2_{temp} + Err^2_{p} + Err^2_{c}} \quad (25)$$

where Err_{temp}, Err_p and Err_c represent the 2σ uncertainties of the measured opacity resulting from variations in temperature, pressure and concentration respectively. The individual uncertainties are obtained by halving the difference between the maximum and minimum of the modeled opacity. For measurements of SO_2/CO_2 mixtures, the model for opacity of SO_2 in a CO_2 atmosphere from Suleiman et al. (1996) was used with upper and lower limits for temperature, pressure and concentration to calculate Err_{cond}, since that model closely fits the measured opacities. Similarly, for measurements of pure CO_2, the model for CO_2 opacity from Ho et al. (1966) was used with upper and lower limits for temperature, pressure, and concentration to calculate Err_{cond}. Thus when evaluating the quality-of-fit of any opacity model (such as in Figs. 3–9 below),

Table 1
Instruments used and associated precision.

Instrument	Range (°C)	Measurement parameter	Precision (3σ)
Omega® PX1009L0-1.5KAV	−18.3 to 343.3	Pressure (0–1500 psia)	±0.25% FS
Omega® PRCU-10-2-100-1/4-9-E	−50 to 450	Temperature (−200 to 400 °C)	±(0.15 + 0.002 rdg) °C
Omega® DP41B	0–50	Temperature (−200 to 900 °C)	±0.2% °C
Agilent® E5071C	~20	*S* parameters	See Hanley et al. (2009)
HP® 34401A multimeter	~20	Voltage (output from transducer)	±(0.0050% rdg + 0.0035% range)
GE Sensing®/Druck® DPI-104	−10 to 50	Pressure (0–30 psia)	±0.05% FS
GE Sensing®/Druck® DPI-104	−10 to 50	Pressure (0–300 psia)	±0.05% FS

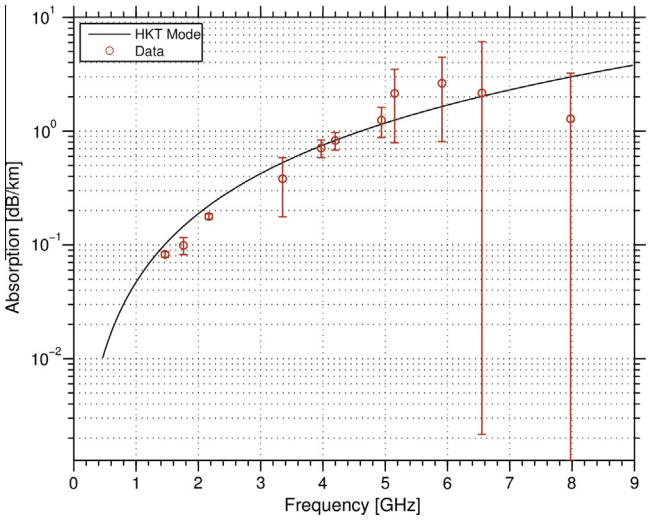

Fig. 3. Measured microwave opacity of pure CO_2 at pressure 79.95 bars and 435.4 K compared with model from Ho et al. (1966). Displayed error bars are 2-sigma.

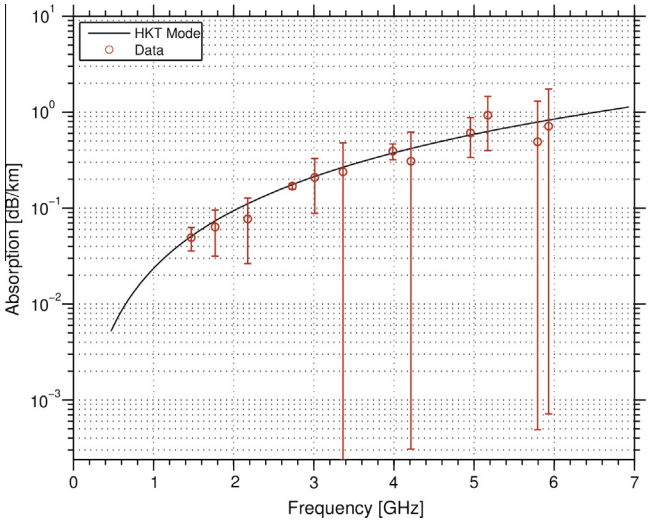

Fig. 4. Measured microwave opacity of pure CO_2 at pressure 78.05 bars and 495.4 K compared with model from Ho et al. (1966). Displayed error bars are 2-sigma.

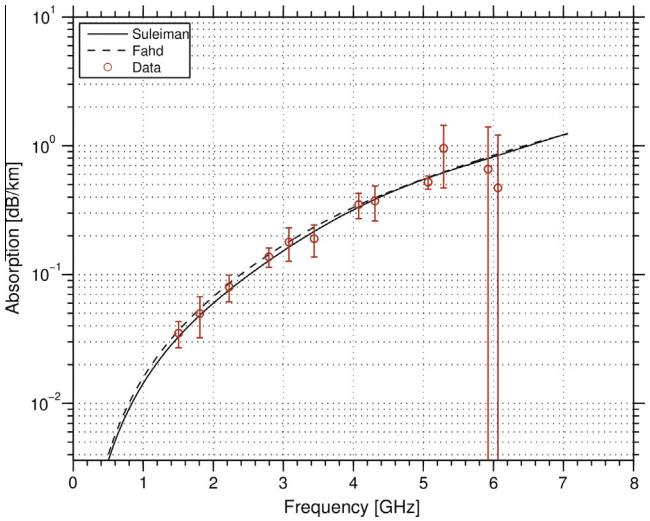

Fig. 5. Measured microwave opacity of pure SO_2 at 492.8 K and 0.260 bars pressure compared with models from Suleiman et al. (1996) and from Fahd and Steffes (1992). Displayed error bars are 2-sigma.

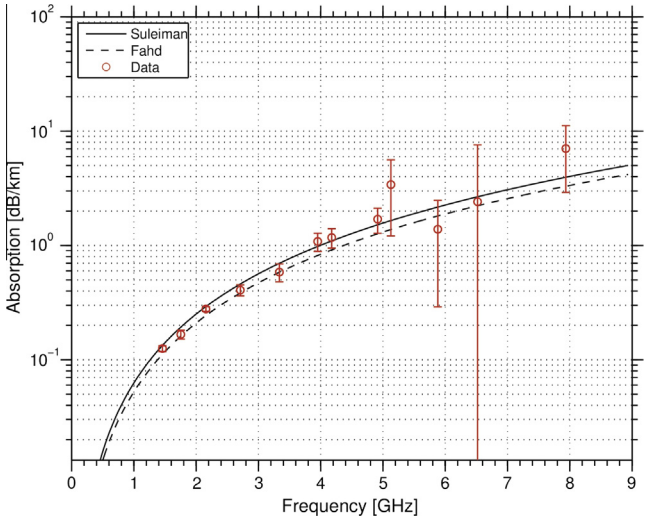

Fig. 6. Measured microwave opacity of SO_2 (0.250 bars, or 0.240% by mole fraction, corrected for compressibility) in a CO_2 atmosphere at 435.3 K and 92.002 bars pressure compared with models from Suleiman et al. (1996) and from Fahd and Steffes (1992). Displayed error bars are 2-sigma.

the effects of Err_{cond} are added as an additional term in Eq. (24) to the measurement uncertainty (Err_{tot}) of each opacity measurement.

3. Measurement results

Two laboratory measurement campaigns (one for pure CO_2 and one for SO_2/CO_2 mixtures) were conducted. In the campaign for pure CO_2, nearly 100 laboratory measurements of microwave opacity were conducted in the pressure range from 20 to 80 bars, at temperatures of 435 and 495 K, and at wavelengths from 3.7 to 20 cm (1.5–8.2 GHz). For the opacity of SO_2 in a CO_2 atmosphere, over 120 laboratory measurements were conducted in the pressure range from 4 to 92 bars; at temperatures of 435 K, 495 K, and 560 K; and at wavelengths from 3.7 to 20 cm (1.5–8.2 GHz). The

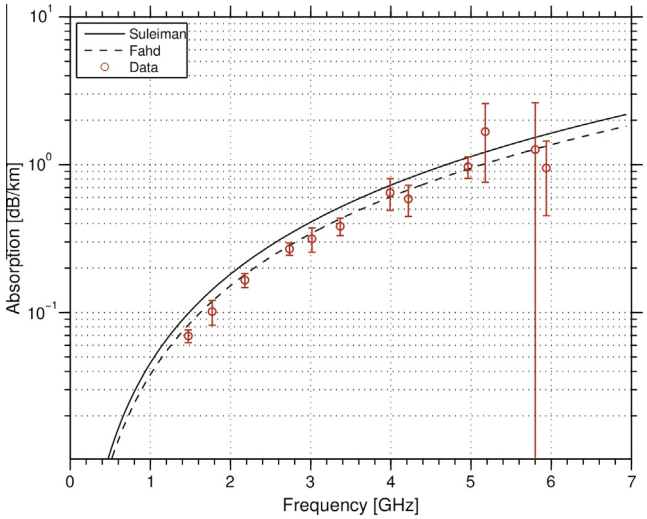

Fig. 7. Measured microwave opacity of SO_2 (0.250 bars, or 0.315% by mole fraction, corrected for compressibility) in a CO_2 atmosphere at 492.8 K and 74.963 bars pressure compared with models from Suleiman et al. (1996) and from Fahd and Steffes (1992). Displayed error bars are 2-sigma.

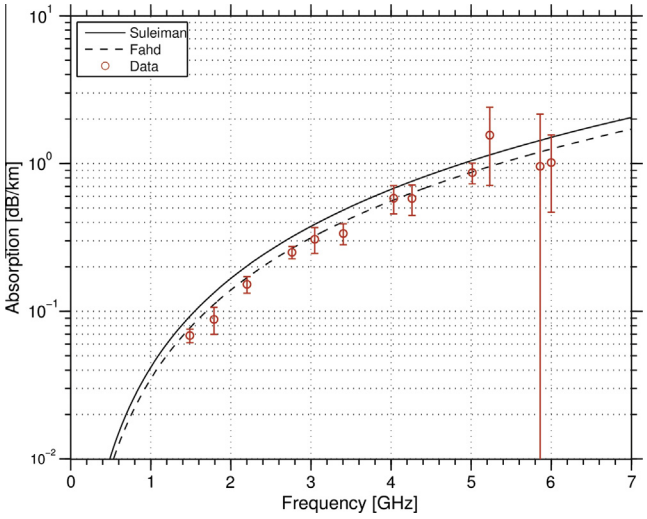

Fig. 8. Measured microwave opacity of SO_2 (0.257 bars, or 0.626% by mole fraction, corrected for compressibility) in a CO_2 atmosphere at 492.8 K and 39.806 bars pressure compared with models from Suleiman et al. (1996) and from Fahd and Steffes (1992). Displayed error bars are 2-sigma.

mole fraction of sulfur dioxide ranged from 0.2% to 7.4% with some additional measurements of pure SO_2. The complete set of processed measurements (with error bars) are included in the online Supplementary Materials section (CO2.xls and SO2CO2.xls).

Typical results for pure CO_2 are shown in Figs. 3 and 4. Results indicate that the model for the centimeter-wavelength opacity from pure CO_2 (developed over 40 years ago – Ho et al., 1966), is valid over the entire centimeter-wavelength range under simulated conditions for the deep atmosphere of Venus. While not an unexpected result, it was important to verify the model over a wider range of temperatures, pressures, and wavelengths since the model from Ho et al. (1966) was based on a single measurement campaign conducted at a single wavelength (3.2 cm).

Typical results for pure SO_2 and for SO_2 in a CO_2 atmosphere are shown in Figs. 5–9. Results indicate that the models for the centimeter-wavelength opacity from SO_2 in a CO_2 atmosphere by Suleiman et al. (1996) and Fahd and Steffes (1992) are valid over the entire centimeter-wavelength range under simulated

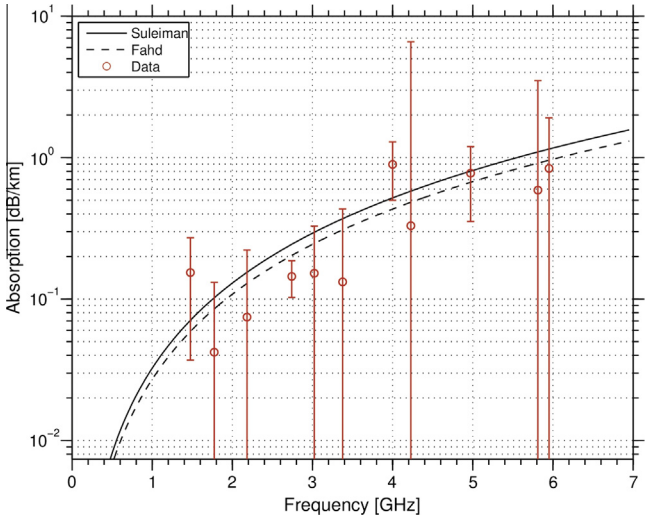

Fig. 9. Measured microwave opacity of SO_2 (0.246 bars, or 0.330% by mole fraction, corrected for compressibility) in a CO_2 atmosphere at 553.1 K and 72.326 bars pressure compared with models from Suleiman et al. (1996) and from Fahd and Steffes (1992). Displayed error bars are 2-sigma.

conditions for the deep atmosphere of Venus. The Fahd and Steffes (1992) model employs the Van Vleck–Weisskopf lineshape, and was developed from measurements of SO_2/CO_2 mixtures conducted at room temperature. As per their paper, we employ only the *rotational* line catalog to compute opacity. (JPL spectral line catalog, Pickett et al., 1998). The Suleiman et al. (1996) model employs the (more complex) Ben Reuven lineshape, and was based on measurements conducted from 290 to 505 K. This model also employs only the *rotational* line catalog to compute opacity. (JPL spectral line catalog, Pickett et al., 1998). Overall, while both models perform well, the Fahd and Steffes (1992) model appears to provide a slightly better fit to the overall data set. (Of the 120 measurements taken of the microwave opacity of SO_2 in a CO_2 atmosphere, the Fahd and Steffes (1992) model fits 83% of the data within the 2-sigma error bars, whereas the Suleiman model fits 63%.) It should also be noted that because both models were derived from measurements conducted at pressures of 6 bars or less, no allowance for the compressibility of CO_2 is included in these models. However, since the compressibility Z, of CO_2 does not deviate from unity by more than 1% over the known Venus temperature/pressure profiles (see e.g., Seiff et al., 1980), both models should perform well at all altitudes in the Venus atmosphere without correction for compressibility. Since some of the high-pressure *laboratory* measurements presented here were conducted at temperatures well below the equivalent Venus temperature for those pressures, and corrections for compressibility were necessary when computing the opacity predicted by the Suleiman et al. (1996) model and by the Fahd and Steffes (1992) model at those temperatures. (These corrections were completed by simply dividing the measured partial pressure of CO_2 by the compressibility, Z, before applying to the models for SO_2 opacity.)

4. Conclusions

Even though based on a limited range of original laboratory measurements, the models for the microwave opacity of pure CO_2 by Ho et al. (1966) and for the microwave opacity of SO_2 in a CO_2 atmosphere from Suleiman et al. (1996) and Fahd and Steffes (1992) have all been shown to be accurate under laboratory conditions similar to the boundary layer of Venus. (We note however, that the Fahd and Steffes (1992) model performs better under these laboratory conditions.) These laboratory measurements are

the first conducted for Venus over an extended centimeter-wavelength range at pressures up to 92 bars. As a result, existing radiative transfer models using these models for microwave opacity (see e.g., Butler et al., 2001; Jenkins et al., 2002; Suleiman, 1998, and Fahd and Steffes, 1992) correctly reflect the roles of these constituents in determining the centimeter-wavelength emission from the Venus boundary layer. Furthermore, these measurements verify the role that centimeter-wavelength emission observations can play in detecting spatial and temporal variations in the temperature and in the abundance of SO_2 in the Venus boundary layer.

Acknowledgments

This work was supported by the NASA Planetary Atmospheres Program under Grant NNX11AD66G. We especially thank Ms. Siri Anne Gomes and Dr. Doug King of Airgas USA for assistance in verifying gas mixture compositions.

Appendix A. Supplementary material

Supplementary data associated with this article can be found, in the online version, at http://dx.doi.org/10.1016/j.icarus.2014.09.012.

References

Butler, B.J., Steffes, P.G., Suleiman, S.H., Kolodner, M.A., Jenkins, J.M., 2001. Accurate and consistent microwave observations of Venus and their implications. Icarus 154, 226–238.

Chinsomboon, G., 2012. New Model for the 5–20 cm Wavelength Opacity of Ammonia Pressure-broadened by Methane under Jovian Conditions based on Laboratory Measurements. MS Thesis, Georgia Institute of Technology, Atlanta, GA.

DeBoer, D.R., Steffes, P.G., 1994. Estimates of the tropospheric vertical structure of Neptune based on microwave radiative transfer studies. Icarus 123, 324–335.

Devaraj, K., 2011. The Centimeter- and Millimeter-Wavelength Ammonia Absorption Spectra under Jovian Conditions. PhD Thesis, Georgia Institute of Technology, Atlanta, GA.

Fahd, A.K., Steffes, P.G., 1992. Laboratory measurements of the microwave and millimeter-wave opacity of gaseous sulfur dioxide (SO_2) under simulated conditions for the Venus atmosphere. Icarus 97, 200–210.

Hanley, T.R., Steffes, P.G., 2007. A high-sensitivity laboratory system for measuring the microwave properties of gases under simulated conditions for planetary atmospheres. Radio Sci. 42 (RS6010), 1–12.

Hanley, T.R., Steffes, P.G., Karpowicz, B.M., 2009. A new model of the hydrogen and helium-broadened microwave opacity of ammonia based on extensive laboratory measurements. Icarus 202, 316–335.

Ho, W., Kaufman, I.A., Thaddeus, P., 1966. Laboratory measurement of microwave absorption in models of the atmosphere of Venus. J. Geophys. Res. 71, 5091–5108.

Jenkins, J.M., Kolodner, M.A., Butler, B.J., Suleiman, S.H., Steffes, P.G., 2002. Microwave remote sensing of the temperature and the distribution of sulfur compounds in the Venus atmosphere. Icarus 158, 312–328.

Karpowicz, B.M., Steffes, P.G., 2011. In search of water vapor on Jupiter: Laboratory measurements of the microwave properties of water vapor under simulated jovian conditions. Icarus 212, 210–223.

Kolodner, M.A., Steffes, P.G., 1998. The microwave absorption and abundance of sulfuric acid vapor in the Venus atmosphere based on new laboratory measurements. Icarus 132, 151–169.

Matthaei, G.L., Young, L., Jones, E., 1980. Microwave Filters, Impedance Matching Networks and Coupling Structures. McGraw-Hill, New York.

Pickett, H.M., Poynter, R.L., Cohen, E.A., Delitsky, M.L., Pearson, J.C., Muller, H.S.P., 1998. Submillimeter, millimeter, and microwave spectral line catalog. J. Quant. Spectrosc. Radiat. Transfer 60, 883–890.

Seiff, A. et al., 1980. Measurements of thermal structure and thermal contrasts in the atmosphere of Venus and related dynamical observations: Results from the four Pioneer Venus probes. J. Geophys. Res. 85, 7903–7933.

Steffes, P.G., Eshleman, V.R., 1981. Laboratory measurements of the microwave opacity of sulfur dioxide and other cloud-related gases under simulated conditions for the middle atmosphere of Venus. Icarus 48, 180–187.

Steffes, P.G., Klein, M.J., Jenkins, J.M., 1990. Observation of the microwave emission of Venus from 1.3 to 3.6 cm. Icarus 84, 83–92.

Steffes, P.G., Devaraj, K., Butler, B.J., 2013. X-band microwave radiometry as a tool for understanding the deep atmosphere of Venus. American Geophysical Union (Fall) 2013, P41D-1954.

Student, 1908. The probable error of a mean. Biometrika 6, 1–25.

Suleiman, S., 1998. Microwave Effects of Gaseous Sulfur Dioxide (SO_2) in the Atmosphere of Venus and Earth. PhD Thesis, Georgia Institute of Technology, Atlanta, GA.

Suleiman, S.H., Kolodner, M.A., Steffes, P.G., 1996. Laboratory measurement of the temperature dependence of gaseous sulfur dioxide (SO_2) microwave absorption with application to the Venus atmosphere. J. Geophys. Res. 101 (E2), 4623–4635.

Tyler, G.L., Howard, H.T., 1969. Refractivity of carbon dioxide under simulated martian conditions. Radio Sci. 4, 899–904.